

E-Beam Nanostructuring and Direct Click Biofunctionalization of Thiol–Ene Resist

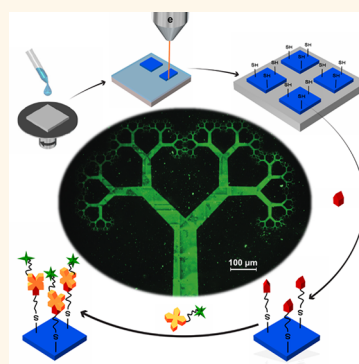
Reza Zandi Shafagh,^{1b} Alexander Vastesson,^{1b} Weijin Guo, Wouter van der Wijngaart,^{*1b} and Tommy Haraldsson

KTH Royal Institute of Technology, Stockholm 10044, Sweden

S Supporting Information

ABSTRACT: Electron beam lithography (EBL) is of major importance for ultraminiaturized biohybrid system fabrication, as it allows combining biomolecular patterning and mechanical structure definition on the nanoscale. Existing methods are limited by multistep biomolecule immobilization procedures, harsh processing conditions that are harmful to sensitive biomolecules, or the structural properties of the resulting protein monolayers or hydrogel-based resists. This work introduces a thiol–ene EBL resist with chemically reactive thiol groups on its native surface that allow the direct and selective “click” immobilization of biomolecules under benign processing conditions. We constructed EBL structured features of size down to 20 nm, and direct functionalized the nanostructures with a sandwich of biotin and streptavidin. The facile combination of polymer nanostructuring with biomolecule immobilization enables mechanically robust biohybrid components of interest for nanoscale biomedical, electronic, photonic, and robotic applications.

KEYWORDS: protein patterning, e-beam, thiol–ene, biohybrid, nanoscale, resist, NEMS



The emerging field of biohybrid systems combines biological and synthetic structural elements for biomedical or robotic applications.^{1,2} The constituting elements of bionanoelectromechanical systems (BioNEMS) are of nanoscale size, for example, DNA, proteins, or nanostructured mechanical parts. This work reports the facile top-down nanostructuring of polymers to create cross-linked and mechanically robust nanostructures that are subsequently functionalized with proteins.

Electron beam lithography (EBL)-based methods allow the direct-write patterning of matter with sub-10 nm resolution. E-beam patterning of protein monolayers, for example, by direct-write inactivation of proteins,³ results in planar structures unsuited as mechanical elements. One strategy toward 3D biofunctionalized nanostructures is the incorporation of proteins in hydrogel-based e-beam resists. Kolodziej and Maynard⁴ review EBL-based patterning of biomolecules with poly(ethylene glycol) (PEG)-based resists. However, these methods suffer from either requirement of complex, multistep surface modification or exposure of proteins to high vacuum and electron radiation conditions not suited for molecules that are prone to denaturation. Bat et al.⁵ describe hydrogel resists of mixtures containing trehalose glycopolymer and proteins, which allow direct-write patterning of multiple proteins by EBL while protecting the proteins from the harsh processing conditions. However, whereas hydrogel resists might be of interest for cell anchoring or cell proliferation applications, they result in poor mechanical properties and make structuring below 100 nm difficult.

A variety of different applications in organic electronics, optics, and biomedicine utilize thiol–ene alternating copolymers because of their tunable mechanical properties, low-stress, low shrinkage, and fast curing process.^{6,7} Previous nanostructuring of thiol–enes, using nanocontact molding,⁸ soft imprint lithography,⁹ step and flash imprint lithography,¹⁰ or UV nanoimprint lithography,¹¹ requires a cumbersome master stamp or mold fabrication and suffers from residual polymer layers and processing imperfections intrinsic to contact-mode processes.^{12,13}

Off-stoichiometric thiol–ene polymers (OSTE)¹⁴ feature reactive thiol groups on their native surface, which can be exploited for rapid one-step microscale surface patterning of biomolecules.¹⁵ Previous OSTE-based devices were shown to be biocompatible¹⁶ and suitable as a substrate for cell growth.¹⁷ The off-stoichiometric formulation also significantly reduces pattern broadening during photostructuring due to diffusion-induced monomer depletion.¹⁸

This work extends direct-write OSTE structuring from photostructured microscale features to e-beam structured nanoscale features with maintained surface reactivity, and demonstrates the direct immobilization of biotin–streptavidin complexes on the native nanostructured surfaces (see Figure 1).

Received: May 17, 2018

Accepted: September 13, 2018

Published: September 13, 2018

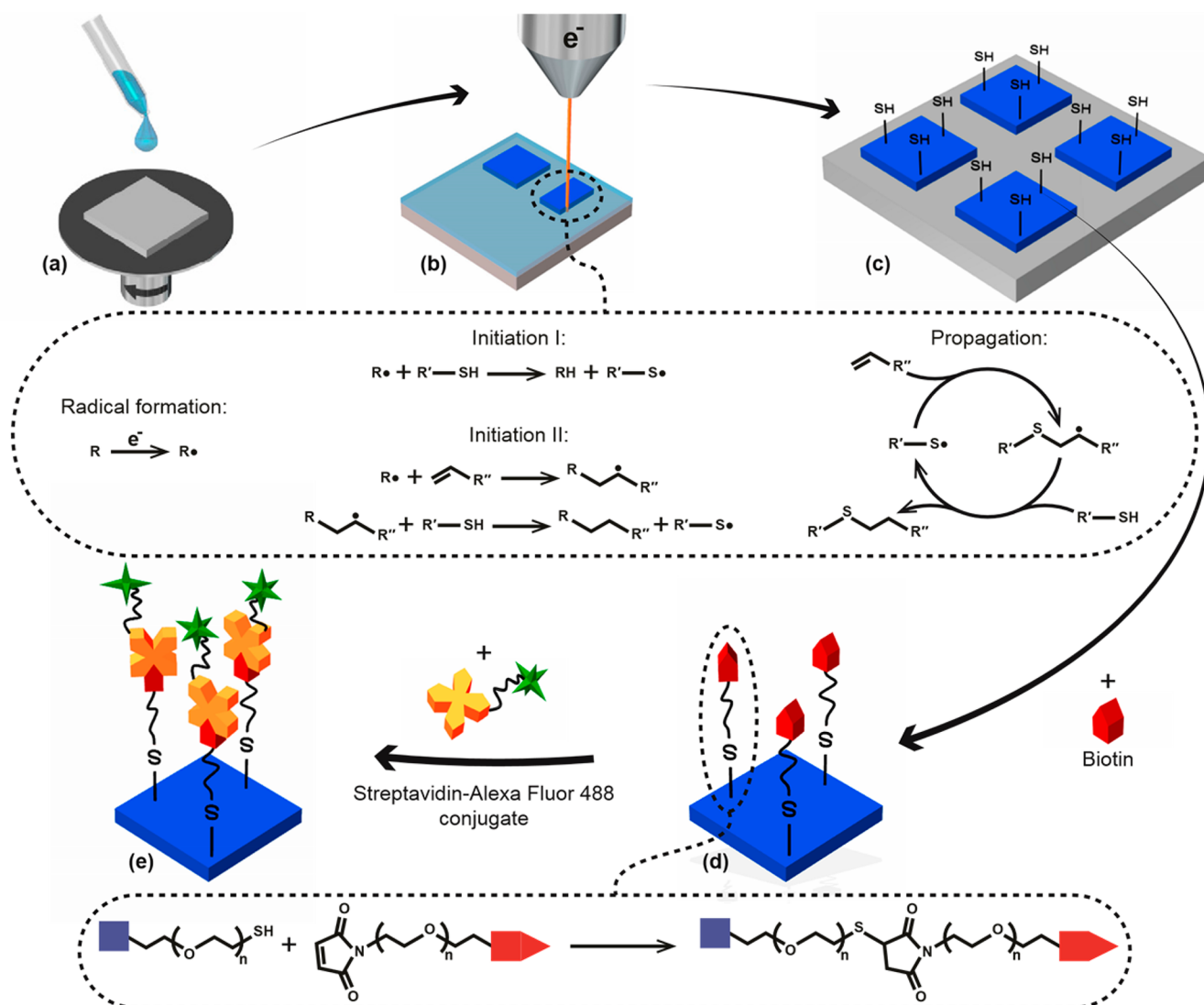


Figure 1. Schematic of the e-beam patterning and direct functionalization of OSTe. (a) Spin coating of OSTe resist. (b) E-beam curing reactions. (c) OSTe structures after patterning expose thiol functional groups on their surfaces. (d) Biotin linkers bind spontaneously to the unreacted thiols on the OSTe surface via thiol-maleimide Michael addition. (e) Fluorescently labeled streptavidin conjugate binds spontaneously to the biotin. OSTe, off-stoichiometric thiol-ene.

Thus, this work introduces three technical key advances. First, direct nanostructuring of thiol-ene copolymers using EBL. Second, e-beam resist that features a chemically reactive surface after patterning. Third, direct covalent (click) biofunctionalization of e-beam resist. The importance of our method lies in the nature of the thiol functionality and its spatial control. Thiol-click chemistry in combination with nanostructuring can be used to achieve an outstanding control of bottom up chemical synthesis,¹⁹ biomolecule immobilization,^{15,20} and nanoscale self-assembly²¹ in a geometrically highly controlled manner. Due to the nature of thiol-click chemistry most processes are performed under benign conditions^{6,19,22} that are compatible with proteins,^{15,20} nucleic acids,²³ and cell cultures.^{17,24,25} The facile structuring and biomolecule immobilization is important for building bio-nanoelectromechanical structures (Bio-NEMS) that can be implemented as, for example, ultraminiaturized sensors or biophotonic transducers.

RESULTS AND DISCUSSION

Figure 2 shows atomic force microscopy (AFM) measurement results of 33 nm thick EBL-structured OSTe resist. The exposed patterns consisted of discs with equidistant diameter and interdistance of 500 and 50 nm, and of lines with equidistant width and interdistance of 250, 100, 50, 30, and 20 nm.

The line edge roughness (LER) increases with decreasing lateral feature size. For feature interdistances of 250 nm or higher, the structure height equals the full OSTe layer thickness and the nonexposed resist is successfully removed from the substrate surface. For smaller interdistances, the structure height is reduced, although features as small as 20 nm remain easily distinguishable. These features are the smallest and most dense reported for thiol-ene polymer networks, regardless of nanopatterning method.

E-beam curing of thiol-ene systems can proceed via free radical polymerization without the use of initiators.^{6,22} However, to achieve micrometer-scale or smaller resolution requires the combination of a high thiol-ene off-stoichiometry

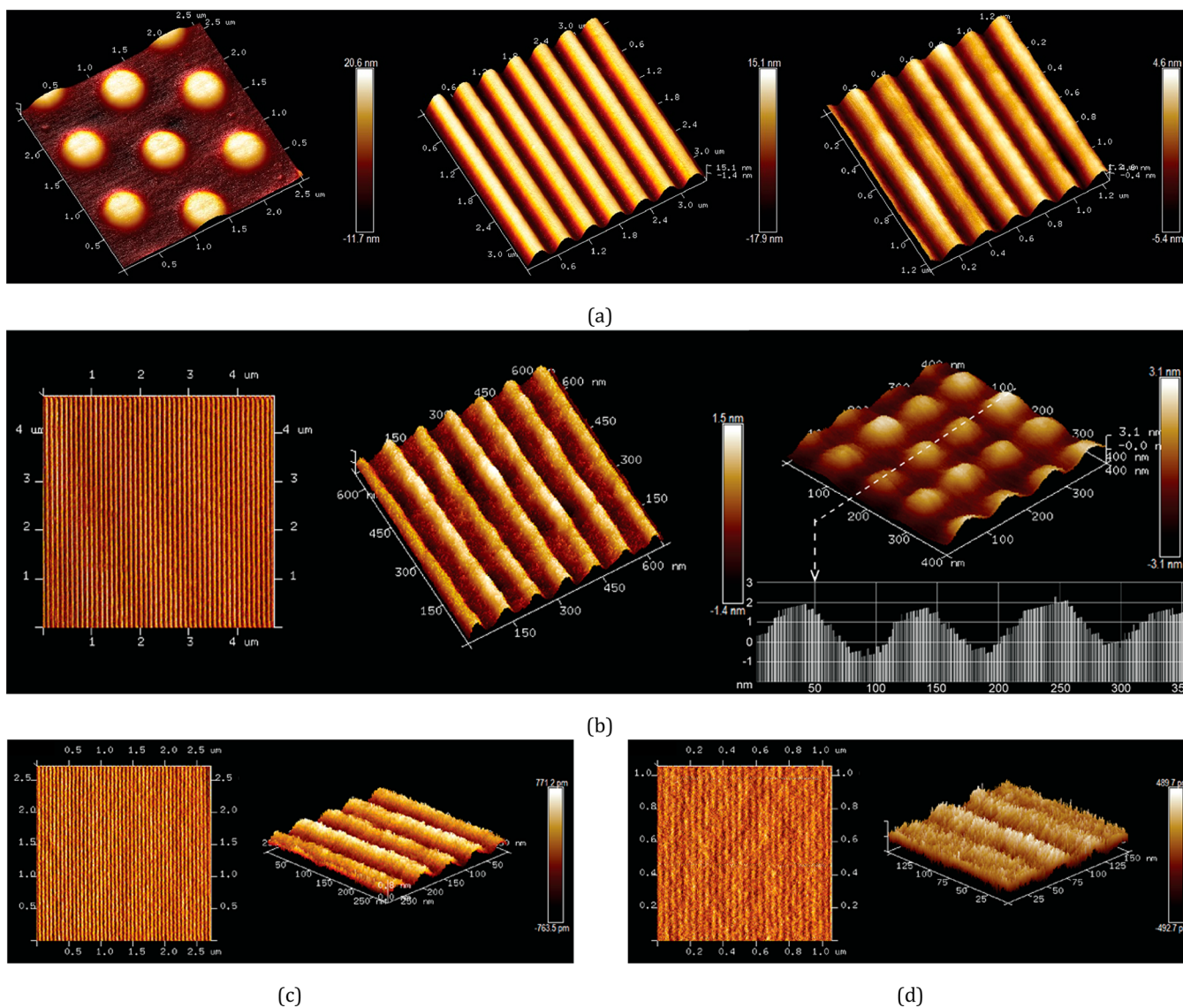


Figure 2. AFM images of gratings and mesa structures of different size, patterned in OSTE via EBL, in which the color bars represent the height of the structures. (a) Circular pillars of 500 nm diameter and half-pitch (left), gratings of 250 nm width and half-pitch (middle), and gratings of 100 nm width and half-pitch (right). (b) Gratings of 50 nm width and half-pitch (left) and circular pillars of 50 nm diameter and half-pitch (right). The dotted white line indicates where the cross-section lays. (c) Gratings of 30 nm width and half-pitch. (d) Gratings of 20 nm width and half-pitch. AFM, atomic force microscopy; EBL, e-beam lithography; OSTE, off-stoichiometric thiol-ene.

and the addition of inhibitor in the resist formulation. Photostructuring of off-stoichiometric thiol-ene prepolymer mixture depletes the deficient monomer in the nonexposed region immediately adjacent to the exposed prepolymer, which suppresses gelation caused by radical diffusion in that region.¹⁸ We hypothesize that a similar effect occurs during e-beam exposure. The addition of inhibitor compound further prohibits the broadening of features by scavenging radicals in nonexposed areas. The high feature density shown in Figure 2 confirms the prevention of feature broadening in the thiol-ene network.

Figure 3 shows a light microscopy image of 5 μm square OSTE resist features after EBL exposure to doses between 100 and 2325 $\mu\text{C}/\text{cm}^2$, followed by development, demonstrating that OSTE EBL resist offers a wide dose window leading to a wide process window, high robustness, and reproducibility. For features of lateral size above 500 nm, the demanded exposure dose ranges from 100 to 500 $\mu\text{C}/\text{cm}^2$. Smaller features require

higher doses of 500–1000 $\mu\text{C}/\text{cm}^2$, which is comparable to the 900–1000 $\mu\text{C}/\text{cm}^2$ dose needed for the widely used negative tone resist HSQ.

Figure S1 shows XPS spectra and elemental states measured on exposed and nonexposed areas of the e-beam resist after development. For exposed areas, resonance peaks at the characteristic binding energy of 163 eV indicate that in average 4.6% of the surface consists of thiol groups.²⁶ We attribute the relatively high nitrogen, high sulfur and low chromium content, when compared to nonexposed areas, to the presence of the thiol monomer $\text{C}_{18}\text{H}_{27}\text{N}_3\text{O}_9\text{S}_3$ in exposed areas, and the uncovering of the underlying substrate in nonexposed areas during development.

The developed e-beam resist has an e-modulus of 3 GPa (Figure S2). This is the highest reported stiffness for off-stoichiometry thiol-enes,²⁷ and substantially stiffer than the respective 130 and 60 MPa stiffness of similar stoichiometric

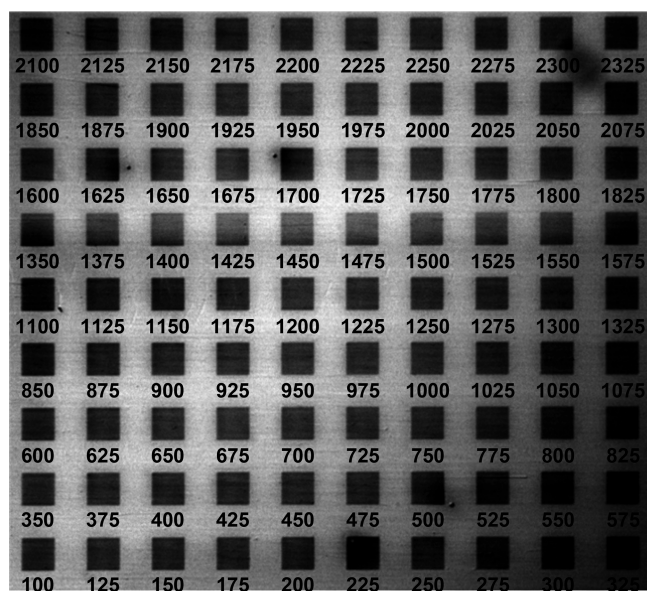


Figure 3. Light microscopy image of $5 \times 5 \mu\text{m}^2$ squares of the OSTE resist after dose testing. The numbers indicate the exposure dose in $\mu\text{C}/\text{cm}^2$.

and off-stoichiometric thiol–ene formulations that were UV-cured.

We speculate that the high degree of stiffening in the e-beam versus UV cured formulations is due to cross-linking via hydrogen abstraction and subsequent bond formation via radical–radical coupling reactions.

Figure 4 shows fluorescence microscopy images of the OSTE resist after EBL, followed by biofunctionalization with biotin and streptavidin–Alexa Fluor 488 conjugate. The exposed patterns consisted of a fractal tree that features a $100 \mu\text{m}$ wide trunk and twigs of width as small as 100 nm ; gratings and arrays of squares and discs of $10 \mu\text{m}$ line size and diameter; and line structures of $50 \mu\text{m}$ length and $250, 500 \text{ nm}$ width with interspacing of 2.5 and $25, 1$ and $50 \mu\text{m}$, respectively.

The fluorescence signal intensity from the OSTE structures is $7.4\times$ higher than that of the control surface (green channel, analyzed by ImageJ). The high fluorescence intensity following the biofunctionalization demonstrates that the thiol–ene resist features chemically reactive thiols on its surface. Thiol reactive groups enable diverse types of biofunctionalization, for example, thiol–gold, thiol–ene, and thiol–Michael addition (click) reactions, with the latter including thiol–maleimide, thiol–vinyl sulfone, thiol–(meth)acrylate, and thiol–yne interactions.²⁸ Here, biotin moieties bind directly and

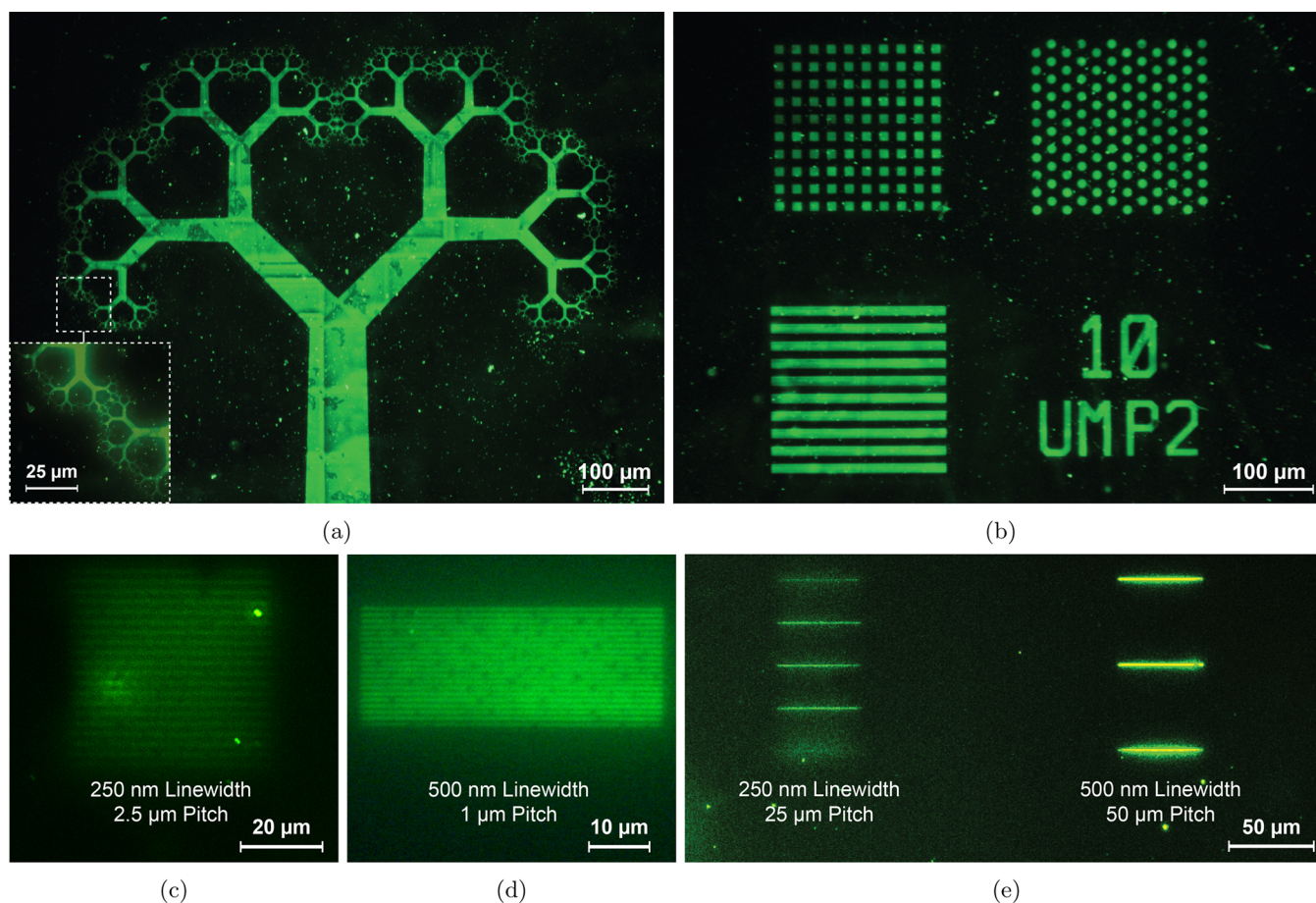


Figure 4. Fluorescence microscopy images of EBL nanopatterned OSTE structures of different size after incubation with biotin and fluorescently labeled streptavidin. (a) Fractal tree shape with microtrunk of width $100 \mu\text{m}$ and branches as small as 100 nm . (b) Dot and line structures with size, line width, and interspacing of $10 \mu\text{m}$. (c) Line structures of $50 \mu\text{m}$ length, with 250 nm width and $2.5 \mu\text{m}$ pitch. (d) Line structures of $50 \mu\text{m}$ length, with 500 nm width and $1 \mu\text{m}$ pitch. (e) Line structures of $50 \mu\text{m}$ length with 250 nm width and $25 \mu\text{m}$ pitch (left); and 500 nm width and $50 \mu\text{m}$ pitch (right). EBL, e-beam lithography; OSTE, off-stoichiometric thiol–ene.

covalently to the e-beam structured OSTE resist surface via a spontaneous thiol–maleimide Michael addition reaction. The subsequent attachment of streptavidin to the immobilized biotin constitutes a full bioassay on top of the e-beam patterned resist.

The lower limit to the protein patterned feature size in this work, 250 nm, is attributed to the requirement of a very fine process window in the development procedure for dense structures. Figure 2 shows the creation of smaller geometrical features, albeit with reduced structural height. This leads us to hypothesize that smaller protein features may be feasible during EBL of thinner OSTE layers, with a thickness comparable to the structural height variations obtained for these smaller line width structures. In addition, tuning the development process with regards to temperature, time and solvent chemistry, along with using higher e-beam energies, may enable more distinct sub-250 nm features.

Our approach has a number of advantages over previous EBL-based in situ protein patterning techniques. We do not expose proteins to the demanding processing conditions inside the e-beam chamber, such as ultrahigh vacuum and high electron energy, widening the possibility of EBL protein patterning to more sensitive proteins. Moreover, our approach obviates multistep surface modifications, such as building SAM layers on top of an e-beam resist or on the underlying substrate.

OSTE is also mechanically more robust, with an E-modulus ~ 3 GPa, compared to the E-moduli of hydrogels, <100 kPa. Due to the nature of thiol-click chemistry most processes can be performed under benign conditions that are compatible with proteins, nucleic acids, and cell cultures. This enables life-science applications, such as the straightforward nanoscale patterning of sensitive biomolecules and small footprint bioassay immobilization.

We hypothesize that in a broader perspective, this work will also enable combining other specific features of OSTE with nanoscale structures, such as the use of thiol-click reactions for direct metal coating, for example, *via* thiol-gold chemistry,²⁹ grafting of functional layers,³⁰ layer bonding,³¹ or component self-assembly; the tuning of the mechanical stiffness, where the previous and current work show E-moduli in the range 2.8 MPa to 3 GPa,^{27,32} and the high and tunable refractive index.³³ The combination of these properties may further lead to potential applications in nanoscale electronic, photonic and robotic systems.

CONCLUSIONS

In conclusion, this work introduces off-stoichiometric thiol–ene copolymers as a new class of e-beam resist. The native surfaces, including the side walls, of the mechanically robust resist structures act as sites for direct and covalent biomolecule immobilization. The results presented here hold specific promises for life-science applications. Combining these results with other features of OSTE materials may further lead to ultraminiaturized biohybrid electronic, photonic and robotic systems.

METHODS

Substrates. As substrate materials, both silicon and fused silica chips coated with 20 nm chromium were used. The thin Cr conductive layer reduces electron charge accumulation in the resist while minimizing the electron backscattering and its subsequent proximity effect.

Preparation of Thiol–Ene Based Precursor Formulations.

(1) The OSTE EBL resist was prepared in three steps. First, 83.2% wt/wt of the trifunctional thiol monomer tris[2-(3-mercaptopropionyloxy)ethyl] isocyanurate (BOC Sciences, USA) and 16.8% wt/wt of the tetra-functional allyl monomer glyoxal bis(diallyl acetal) (Sigma-Aldrich, Germany) were thoroughly mixed using a speed-mixer (Hauschild Engineering, Germany), resulting in a monomer composition with functional group molar ratio trithiol:tetra-allyl of 1.8:1. Second, the thiol–ene resist was diluted in propylene glycol monomethyl ether acetate (Sigma-Aldrich, Germany) to create a solution of concentration 5% wt/wt. Finally, 0.67% wt/wt of an inhibitor solution was added, consisting of 15% wt/wt of Q-1301 (Wako Chemical Inc., Japan) dissolved in tetrahydrofuran (Sigma-Aldrich, Germany). The OSTE EBL resist solution was stored in a dark environment at +4 °C until used.

(2) A new precursor formulation of OSTE for UV curing purposes was prepared by addition of 0.5% wt/wt of 1-hydroxycyclohexyl phenyl ketone (IRG) photoinitiator (Irgacure 184, BASF, Germany) to the same 1.8:1 thiol–ene blend and dilution in the same solvent to obtain a final 5% wt/wt thiol–ene solution.

(3) An on-stoichiometric thiol–ene (ONSTE) formulation for UV curing was prepared by 73.4% wt/wt of the thiolmonomer mixed with 26.6% wt/wt of the allyl monomer. The resulting 1:1 functional group ratio blend was mixed with 0.5% wt/wt of the photoinitiator and diluted in the solvent to reach a 5% wt/wt thiol–ene solution.

The thiol–ene based solutions were stored in a dark environment at +4 °C until used.

Substrate Preparation by Spin-Coating. Thin films of thiol–ene based resists were spin-coated on the substrates at 4000 rpm, with an acceleration of 3000 rpm/s, for 5 s resulting in a 30–50 nm resist thickness, as measured by using a stylus profiler (KLA-Tencor P-15, Milpitas). The high spin acceleration rate was used to ensure a uniform film coating of OSTE.

E-Beam Patterning. E-beam writing was performed (Raith 150, Germany) at an exposure voltage of 25 keV. Different exposure doses in the range 100–2325 $\mu\text{C}/\text{cm}^2$ were applied, depending on the targeted resolution.

Different features were e-beam patterned, including gratings and arrays of circular and square pillars with feature size between 20 nm and 10 μm . We also patterned a single fractal structure containing features of size ranging from 100 nm to 100 μm .

UV Curing. The precursors adapted for UV curing were exposed to collimated (3° collimation half angle) near UV short-arc mercury lamp (OAI, Milpitas) at 10.5 mW cm^{-2} for 10 s.

Development. Samples were developed by immersion into hexyl acetate (Sigma-Aldrich, Germany) for 30 s at room temperature.

XPS Analysis. To measure the relative concentration of the thiol functional group next to the e-beam exposure, an e-beam structured chip containing OSTE patterns was characterized by XPS (VersaProbeIII Scanning XPS microprobe, monochromatic Al $K\alpha$ source ($h\nu = 1486.6$ eV), Beam size: 50 μm). Five positions on both e-beam structured and nonexposed areas were selected for XPS analysis (see Figure S2).

Protein Functionalization. A solution of 10 mM maleimide-PEG2-biotin (ThermoFisher, Sweden) in PBS (ThermoFisher, Sweden) was incubated on the structured OSTE surface for 10 min, followed by rinsing with PBS containing 0.05% Tween 20 (VWR Chemicals, Sweden). Thereafter, streptavidin solution (Alexa Fluor 488 conjugate, 12 μM in PBS, ThermoFisher, Sweden) was incubated on the sample for 10 min, followed by rinsing with PBS containing 0.05% Tween 20 and pure PBS in sequence, and drying at room temperature.

Microscopy. Structures were evaluated by light microscopy, atomic force microscopy (AFM, from Bruker ICON) using noncontact mode, and fluorescence microscopy (Nikon, Japan).

Elastic Modulus Analysis. Two samples entirely coated by thin films of UV cured on-stoichiometric thiol–ene and OSTE 80%, along with an additional sample containing e-beam structured patterns of OSTE 80% were quantitatively inspected using the same AFM microscopy equipped with a multifrequency lock-in amplifier (MLA

hardware) and Intermodulation AFM software suite (Intermodulation Products AB, Sweden). E-modulus quantification was done through DMT-EXP model.³⁴

ASSOCIATED CONTENT

Supporting Information

The Supporting Information is available free of charge on the ACS Publications website at DOI: 10.1021/acsnano.8b03709.

XPS analysis data and intermodulation AFM analysis data (PDF)

AUTHOR INFORMATION

Corresponding Author

*E-mail: wouter@kth.se.

ORCID

Reza Zandi Shafagh: 0000-0003-4322-6192

Alexander Vastesson: 0000-0001-9651-4900

Wouter van der Wijngaart: 0000-0001-8248-6670

Notes

The authors declare no competing financial interest.

ACKNOWLEDGMENTS

We thank Dr. Ronnie Jansson and Dr. My Hedhammar at KTH for the opportunity to use their fluorescence microscope.

REFERENCES

- (1) Freudenberg, U.; Liang, Y.; Kiick, K. L.; Werner, C. Glycosaminoglycan-based Biohybrid Hydrogels: A Sweet and Smart Choice for Multifunctional Biomaterials. *Adv. Mater.* **2016**, *28*, 8861–8891.
- (2) Yoon, J.; Eyster, T. W.; Misra, A. C.; Lahann, J. Cardiomyocyte-driven Actuation in Biohybrid Microcylinders. *Adv. Mater.* **2015**, *27*, 4509–4515.
- (3) Rundqvist, J.; Mendoza, B.; Werbin, J. L.; Heinz, W. F.; Lemmon, C.; Romer, L. H.; Haviland, D. B.; Hoh, J. H. High Fidelity Functional Patterns of an Extracellular Matrix Protein by Electron Beam-based Inactivation. *J. Am. Chem. Soc.* **2007**, *129*, 59–67.
- (4) Kolodziej, C. M.; Maynard, H. D. Electron-beam Lithography for Patterning Biomolecules at the Micron and Nanometer Scale. *Chem. Mater.* **2012**, *24*, 774–780.
- (5) Bat, E.; Lee, J.; Lau, U. Y.; Maynard, H. D. Trehalose Glycopolymer Resists Allow Direct Writing of Protein Patterns by Electron-beam Lithography. *Nat. Commun.* **2015**, *6*, 6654.
- (6) Hoyle, C. E.; Lee, T. Y.; Roper, T. Thiolenes: Chemistry of the past with Promise for the Future. *J. Polym. Sci., Part A: Polym. Chem.* **2004**, *42*, 5301–5338.
- (7) Ashley, J. F.; Cramer, N. B.; Davis, R. H.; Bowman, C. N. Soft-lithography Fabrication of Microfluidic Features Using Thiol-ene Formulations. *Lab Chip* **2011**, *11*, 2772–2778.
- (8) Hagberg, E. C.; Malkoch, M.; Ling, Y.; Hawker, C. J.; Carter, K. R. Effects of Modulus and Surface Chemistry of Thiol-ene Photopolymers in Nanoimprinting. *Nano Lett.* **2007**, *7*, 233–237.
- (9) Campos, L. M.; Meinel, I.; Guino, R. G.; Schierhorn, M.; Gupta, N.; Stucky, G. D.; Hawker, C. J. Highly Versatile and Robust Materials for Soft Imprint Lithography Based on Thiol-ene Click Chemistry. *Adv. Mater.* **2008**, *20*, 3728–3733.
- (10) Khire, V. S.; Yi, Y.; Clark, N. A.; Bowman, C. N. Formation and Surface Modification of Nanopatterned Thiol-ene Substrates Using Step and Flash Imprint Lithography. *Adv. Mater.* **2008**, *20*, 3308–3313.
- (11) Lin, H.; Wan, X.; Jiang, X.; Wang, Q.; Yin, J. a Nanoimprint Lithography Hybrid Photoresist Based on the Thiolene System. *Adv. Funct. Mater.* **2011**, *21*, 2960–2967.
- (12) Ahn, S. H.; Guo, L. J. Large-area Roll-to-roll and Roll-to-plate Nanoimprint Lithography: A Step Toward High-throughput

Application of Continuous Nanoimprinting. *ACS Nano* **2009**, *3*, 2304–2310.

(13) Malloy, M.; Litt, L. C. Technology Review and Assessment of Nanoimprint Lithography for Semiconductor and Patterned Media Manufacturing. *J. Micro/Nanolithogr., MEMS, MOEMS* **2011**, *10*, 032001.

(14) Carlborg, C. F.; Haraldsson, T.; Oberg, K.; Malkoch, M.; Van Der Wijngaart, W. Beyond Pdms: Off-stoichiometry Thiol-ene (Oste) Based Soft Lithography for Rapid Prototyping of Microfluidic Devices. *Lab Chip* **2011**, *11*, 3136–3147.

(15) Lafleur, J. P.; Kwapiszewski, R.; Jensen, T. G.; Kutter, J. P. Rapid Photochemical Surface Patterning of Proteins in Thiol-ene Based Microfluidic Devices. *Analyst* **2013**, *138*, 845–849.

(16) Ejserholm, F.; Stegmayr, J.; Bauer, P.; Johansson, F.; Wallman, L.; Bengtsson, M.; Oredsson, S. Biocompatibility of a Polymer Based on Off-stoichiometry Thiol-enes+Epoxy (Oste+) for Neural Implants. *Biomater. Res.* **2015**, *19*, 19.

(17) Sticker, D.; Rothbauer, M.; Lechner, S.; Hehenberger, M.-T.; Ertl, P. Multi-layered, Membrane-integrated Microfluidics Based on Replica Molding of a Thiol-ene Epoxy Thermoset for Organ-on-a-chip Applications. *Lab Chip* **2015**, *15*, 4542–4554.

(18) Hillmering, M.; Pardon, G.; Vastesson, A.; Supekar, O.; Carlborg, C. F.; Brandner, B. D.; Van Der Wijngaart, W.; Haraldsson, T. Off-stoichiometry Improves the Photostructuring of Thiolenes Through Diffusion-induced Monomer Depletion. *Microsyst. Nanoeng.* **2016**, *2*, 15043.

(19) Hoyle, C. E.; Lowe, A. B.; Bowman, C. N. Thiol-click Chemistry: A Multifaceted Toolbox for Small Molecule and Polymer Synthesis. *Chem. Soc. Rev.* **2010**, *39*, 1355–1387.

(20) Hoffmann, C.; Pinelo, M.; Woodley, J. M.; Daugaard, A. E. Development of a Thiolene Based Screening Platform for Enzyme Immobilization Demonstrated Using Horseradish Peroxidase. *Bio-technol. Prog.* **2017**, *33*, 1267–1277.

(21) Groschel, A. H.; Muller, A. H. E. Self-assembly Concepts for Multicompartment Nanostructures. *Nanoscale* **2015**, *7*, 11841–11876.

(22) Hoyle, C. E.; Bowman, C. N. Thiolene Click Chemistry. *Angew. Chem., Int. Ed.* **2010**, *49*, 1540–1573.

(23) Kwak, M.; Herrmann, A. Nucleic Acid/Organic Polymer Hybrid Materials: Synthesis, Superstructures, and Applications. *Angew. Chem., Int. Ed.* **2010**, *49*, 8574–8587.

(24) Sawicki, L. A.; Kloxin, A. M. Design of Thiol-ene Photoclick Hydrogels Using Facile Techniques for Cell Culture Applications. *Biomater. Sci.* **2014**, *2*, 1612–1626.

(25) Sticker, D.; Lechner, S.; Jungreuthmayer, C.; Zanghellini, J.; Ertl, P. Microfluidic Migration and Wound Healing Assay Based on Mechanically Induced Injuries of Defined and Highly Reproducible Areas. *Anal. Chem.* **2017**, *89*, 2326–2333.

(26) Wagner, C. D.; Riggs, W. M.; Davis, L. E.; Moulder, J.; Muilenberg, G. E. *Handbook of X-ray Photoelectron Spectroscopy: A Reference Book of Standard Data for Use in X-ray Photoelectron Spectroscopy*; Perkin-Elmer Corp.: Eden Prairie, MN, 1979.

(27) Sandström, N.; Shafagh, R. Z.; Vastesson, A.; Carlborg, C. F.; van der Wijngaart, W.; Haraldsson, T. Reaction Injection Molding and Direct Covalent Bonding of Oste+ Polymer Microfluidic Devices. *J. Micromech. Microeng.* **2015**, *25*, 075002.

(28) Nair, D. P.; Podgorski, M.; Chatani, S.; Gong, T.; Xi, W.; Fenoli, C. R.; Bowman, C. N. the Thiol-michael Addition Click Reaction: A Powerful and Widely Used Tool in Materials Chemistry. *Chem. Mater.* **2014**, *26*, 724–744.

(29) Rahiminejad, S.; Hansson, J.; Köhler, E.; van der Wijngaart, W.; Haraldsson, T.; Haasl, S.; Enoksson, P. Rapid Manufacturing of OSTE Polymer RF-MEMS Components. *Proceedings of the IEEE 30th International Conference on Microelectromechanical Systems (MEMS)* **2017**, 901–904.

(30) Pardon, G.; Saharil, F.; Karlsson, J. M.; Supekar, O.; Carlborg, C. F.; van der Wijngaart, W.; Haraldsson, T. Rapid Moldfree Manufacturing of Microfluidic Devices with Robust and Spatially

Directed Surface Modifications. *Microfluid. Nanofluid.* **2014**, *17*, 773–779.

(31) Saharil, F.; Carlborg, C. F.; Haraldsson, T.; Van Der Wijngaart, W. Biocompatible "Click" Wafer Bonding for Microfluidic Devices. *Lab Chip* **2012**, *12*, 3032–3035.

(32) Hansson, J.; Karlsson, J. M.; Carlborg, C. F.; van der Wijngaart, W.; Haraldsson, T. Low Gas Permeable and Non-absorbent Rubbery OSTE For Pneumatic Microvalves. *Proceedings of the IEEE 27th International Conference on Microelectromechanical Systems (MEMS)* **2014**, 987–990.

(33) Hata, E.; Tomita, Y. Stoichiometric Thiol-to-ene Ratio Dependences of Refractive Index Modulation and Shrinkage of Volume Gratings Recorded in Photopolymerizable Nanoparticle-polymer Composites Based Onstep-growth Polymerization. *Opt. Mater. Express* **2011**, *1*, 1113–1120.

(34) Forchheimer, D.; Platz, D.; Tholen, E. a.; Haviland, D. B. Model-based Extraction of Material Properties in Multifrequency Atomic Force Microscopy. *Phys. Rev. B: Condens. Matter Mater. Phys.* **2012**, *85*, 195449.